Design of Compressed Truncated Perfect Nozzles

Joe D. Hoffman*

Purdue University, West Lafayette, Indiana

An analysis is presented for designing and predicting the performance of compressed truncated perfect nozzles. A study was performed to determine the relative merits of such nozzles compared to Rao nozzles. It was found that Rao nozzles always yield higher performance than compressed truncated perfect nozzles. However, the performance differences are quite small (0.04-0.34%), which shows that compressed truncated perfect nozzles are good propulsive nozzles. For nozzle envelopes for which the Rao nozzle design concept fails, compressed truncated perfect nozzles may yield very efficient nozzle designs.

Nomenclature

C_D = discharge coefficient
F = thrust
F_{IVL} = initial-value line thrust
F_{SS} = supersonic contour thrust
I_{sp} = specific impulse
L = nozzle length
$\dot{m}$ = mass flow rate
M_D = perfect nozzle design Mach number
P_a = ambient pressure
P_t = stagnation pressure
R = gas constant
T_t = stagnation temperature
y_e = exit radius
y_t = throat radius
γ = gas specific heat ratio
ϵ_D = perfect nozzle design area ratio
θ_a = throat initial expansion angle
ρ_{td} = throat downstream radius of curvature
ρ_{tu} = throat upstream radius of curvature

Introduction

Several methods are employed for designing the diverging contour of axisymmetric converging-diverging propulsive nozzles. The simplest contour is a conical contour. Conical nozzles generally have unacceptable performance losses due to large flow divergence. These losses can be reduced by using contoured diverging sections that turn the flow back toward the axial direction. Circular arc and parabolic contours are commonly used for that purpose.

Several maximum thrust nozzle design procedures have been developed to further reduce the divergence losses. One of the most popular methods, based on a calculus of variations analysis, was developed by Rao.[1] Such nozzles are called Rao nozzles.

An alternate procedure is to design a parallel uniform exit flow nozzle, called a perfect nozzle, and to truncate that nozzle at a much shorter length. Ahlberg, Hamilton, Migdal, and Nilson[2] present some results obtained by this method. While this approach does yield fairly high performance, such truncated perfect nozzles always yield lower performance than Rao nozzles having the same length and area ratio.

Gogish[3] has suggested a design procedure in which truncated perfect nozzles are linearly compressed to yield extremely short nozzles. He suggests that such compressed truncated perfect nozzles may have higher performance than a Rao nozzle designed for the same envelope (i.e., the same length and area ratio). The object of the present investigation was to develop a method for designing compressed truncated perfect nozzles and to develop a procedure for predicting the performance of such nozzles.

Compressed Nozzle Design

There are three steps in the design of a compressed truncated perfect nozzle contour. The first step is to design a perfect nozzle contour for a specified area ratio. The second step is to truncate the perfect nozzle contour at a specified area ratio smaller than its design area ratio. The third step is to compress the truncated perfect nozzle contour to the desired length. These procedures are described in this section.

Perfect Nozzle Design

The design of a perfect nozzle for a specified area ratio is a straightforward procedure. Zucrow and Hoffman[4] discuss this procedure in detail. The essential features of a perfect nozzle are illustrated in Fig. 1. The inlet and initial expansion contours must be prespecified. The subsonic/transonic flowfield in the nozzle inlet and throat region must be calculated. For conventional nozzle throat sections employing a circular arc throat contour, the method developed by Kliegel and Levine[5] is adequate. For more complicated throat sections, a method such as VNAP2 developed by Cline[6] may be required.

In either case, once the transonic solution has been calculated, the method of characteristics[7] is used to calculate the initial expansion flowfield determined by the throat downstream contour. Right-running Mach lines are originated from prespecified points along contour *TA* and extended to the nozzle axis. Thus, the Mach number distribution along the axis is determined. The flow leaving the nozzle is a parallel uniform flow with the Mach number M_D corresponding to the specified area ratio ϵ_D. The point on the nozzle axis where M_D occurs is located, and a straight left-running Mach line is projected from that point to locate the nozzle exit point, point *E*. The flowfield in the turning region is calculated by the method of characteristics. The turning contour itself is located in this flowfield by performing a mass balance along the rearward projected right-running Mach lines. This procedure must be repeated for each area ratio of interest, thus generating a family of perfect nozzle designs.

Compressed Nozzle Design

A compressed truncated perfect nozzle contour is obtained by truncating the perfect nozzle contour and linearly com-

pressing the truncated perfect nozzle contour in the axial direction to obtain the desired nozzle length. This procedure is illustrated in Fig. 2.

The turning contour of the perfect nozzle attaches smoothly to the circular arc initial-expansion contour at point A, as illustrated in Fig. 2, which illustrates the perfect nozzle, the truncated perfect nozzle, and the compressed truncated perfect nozzle. The turning contour is compressed linearly by the compression factor C, given by

$$C = \frac{(x_{e''} - x_a)}{(x_{e'} - x_a)} \qquad (1)$$

The compression factor C is applied to every point along the truncated perfect nozzle contour to obtain a compressed nozzle contour.

The above compression procedure creates a discontinuity in the nozzle wall slope at the attachment point, point A, as illustrated in Fig. 3. This discontinuity is eliminated by shifting the compressed contour downstream until the compressed contour is tangent to the circular arc initial-expansion contour. The amount of axial shifting required is denoted by Δx_s. This shifting must be applied to the entire compressed nozzle contour. The attachment point between the initial-expansion contour and the turning contour also shifts from point A to point A', which has a larger angle.

The above procedure yields a nozzle which has a more rapid initial expansion followed by a more severe turn back, as compared to the truncated perfect nozzle. Consequently, strong right-running compression waves propagate from the compressed contour into the flowfield. If the compression is strong enough, the Mach lines will coalesce and form a right-running oblique shock wave, as illustrated in Fig. 4. The shock wave will increase the static pressure as the flow crosses the shock wave. If the shock wave lies near the nozzle wall, the pressure along the wall will be increased, thus increasing the nozzle thrust. This effect is the mechanism by which the compressed nozzle may yield higher performance than a Rao nozzle.

Flowfield Model

The general features of the flowfield in the compressed nozzle are illustrated in Fig. 4. The flow is assumed to originate upstream of the nozzle in a uniform flow region having constant stagnation pressure and temperature. The flowing fluid is assumed to be a thermally and calorically perfect gas (i.e., constant molecular weight and specific heats). The presence of condensed phases and chemical reactions is neglected, and boundary layer effects are considered negligible. Consequently, the flowfield is isentropic everywhere except across the oblique shock wave, which is described by the standard oblique shock wave relationships.

The flowfield in the transonic region and the supersonic region upstream of the shock wave is irrotational (i.e., constant entropy and stagnation enthalpy throughout) since the flow originates in a uniform flow region and is isentropic. The flowfield downstream of the oblique shock wave is rotational due to the entropy gradient produced by the curved oblique shock wave.

The flowfield in the throat region of the nozzle is assumed to be completely specified by the perturbation analysis developed by Kliegel and Levine,[5] which depends only on the geometry of the nozzle throat. From this analysis, the flow properties along an initial-value line, line TT', spanning the nozzle throat are determined.

Right-running Mach lines are then originated from each point along initial-value line TT', starting with the points adjacent to the axis. These right-running Mach lines are continued until they intersect the nozzle axis. The last such right-running Mach line, line TT'', emanating from the nozzle throat wall point defines the extent of the initial-value problem. Right-

running Mach line TT'' is the control right-running Mach line for the procedure discussed below.

Left-running Mach lines are then originated from points on control right-running Mach line TT'', starting at the first point adjacent to the nozzle throat point T, and continued until they reach the nozzle throat downstream radius of curvature, contour TA'. This process is continued from succeeding points on control right-running Mach line TT'' until the entire region adjacent to the nozzle throat downstream circular arc, contour TA', has been determined.

Left-running Mach lines are then originated from the remaining points along control right-running Mach line TT'' and continued until they intersect the nozzle wall, contour $A'E''$. This process is continued until either the first point on the oblique shock wave is reached (point S), or point T'', which lies on the nozzle axis, is reached. In the latter case, left-running Mach lines are emanated from the nozzle axis and continued across the flowfield. In either case, a left-running Mach line will eventually reach the first point on the oblique shock wave, point S.

A right-running oblique shock wave forms at point S. That right-running oblique shock wave propagates into the flowfield and intersects the left-running Mach lines as they propagate toward the wall. The flowfield up to the shock wave is irrotational, and the flowfield downstream of the shock wave is rotational. The flow property changes across the oblique shock wave depend on the strength of the shock wave, which is determined by both the upstream flowfield and the downstream flowfield. After passing through the oblique shock wave, the left-running Mach lines continue until they intersect the nozzle wall. This process is continued until the end of the nozzle, point E'', is reached.

The flowfield model described above is based on the assumption that the location of point S, the point where the oblique shock wave originates, is known. That point must be predetermined by first constructing the network of left-running Mach lines without a shock wave and locating the point in the characteristic network where right-running Mach lines coalesce. The coalescence of right-running Mach lines indicates the formation of a right-running oblique shock wave.

Nozzle Performance

The performance of a propulsive nozzle is specified by its mass flow rate $\dot{m}$, thrust F, and specific impulse I_{sp}. The nozzle performance model is presented in this section.

The flowfield in the throat region was predicted by the perturbation analysis developed by Kliegel and Levine.[5] From

Table 1   Parameters employed in the parametric studies

Gas specific heat ratio γ	1.2155
Gas constant R, (ft-lbf)/(lbm-R)	68.1753
Stagnation pressure P_t, lbf/in.^{2}	1500.00
Stagnation temperature T_t, R	6131.25
Ambient pressure P_a, lbf/in.^{2}	0.0
Throat radius y_t, in.	1.0
Throat upstream radius of curvature ρ_{tu}, in.	1.0
Throat downstream radius of curvature ρ_{td}, in.	2.0

Table 2   Rao nozzle geometric properties and performance

Parameter	Nozzle 1	Nozzle 2	Nozzle 3
Nominal area ratio ϵ	400	200	100
Exact area ratio ϵ	400	190.43	97.32
Length L, in.	60.189	38.255	24.567
Exit lip radius y_e, in.	20.000	13.800	9.865
Throat attachment angle θ_a, deg	39.833	38.000	37.000
Mass flow rate $\dot{m}$, lbm/s	26.672	26.672	26.672
Thrust F, lbf	9297.8	9102.9	8893.4
Specific impulse I_{sp}, (lbf-s)/lbm	348.60	341.29	333.45
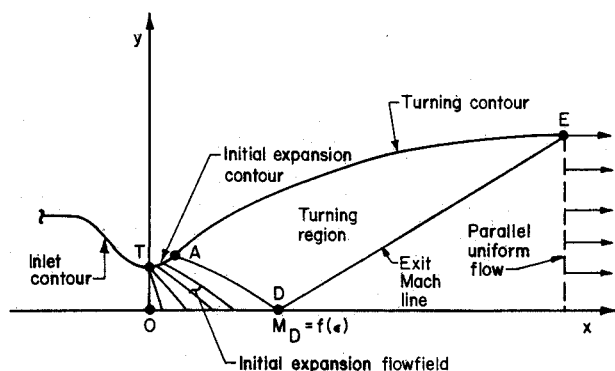
Fig. 1 Basic components of a perfect nozzle.

Fig. 2 Compressed nozzle design.

Fig. 3 Attachment point analysis.

Fig. 4 Schematic illustration of nozzle flowfield.
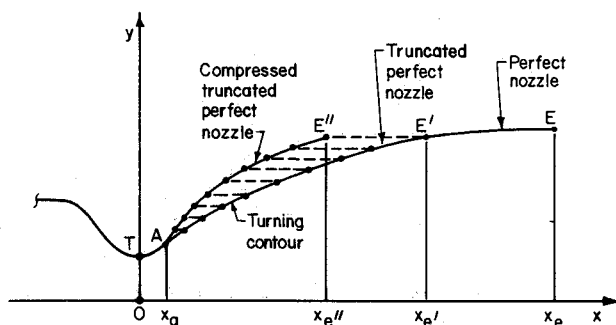
that analysis, an initial-value line was obtained from which the supersonic flowfield can be calculated. In addition, the nozzle mass flow rate $\dot{m}$, discharge coefficient C_D, and initial-value line thrust F_{IVL} were obtained.

The flowfield in the supersonic region was calculated by the method of characteristics for steady two-dimensional supersonic flow. From that analysis, the pressure acting along the wall is known at each point where a Mach line intersects the wall. The thrust developed along the supersonic expansion contour was obtained by integrating (numerically) the axial component of the force developed by the pressure acting on the wall. Thus,

$$F_{\text{SS}} = \int_{y_t}^{y_e} (P - P_a) 2\pi y \, dy \qquad (2)$$

The total thrust developed by the nozzle, F_N, is the sum of the thrust developed across the initial-value line, F_{IVL}, and the thrust developed along the supersonic contour, F_{SS}. Thus,

$$F_N = F_{\text{IVL}} + F_{\text{SS}} \qquad (3)$$

The nozzle specific impulse is given by

$$I_{\text{sp}} = F_N / \dot{m} \qquad (4)$$

Parametric Study

A parametric study was conducted to investigate the potential of compressed truncated perfect nozzles for use as propulsive nozzles. Three different Rao nozzles were designed, with nominal area ratios of 400, 200, and 100. These Rao nozzles were considered as the reference designs for the parametric study. A set of perfect nozzles was designed having area ratios from 97.32 to 800. These perfect nozzles were truncated at the area ratios of the three Rao nozzles and compressed to the length of the Rao nozzles. The performance of these compressed truncated perfect nozzles was compared to the performance of the Rao nozzles. The performance of a 15-deg conical nozzle and three conical nozzles fit to the
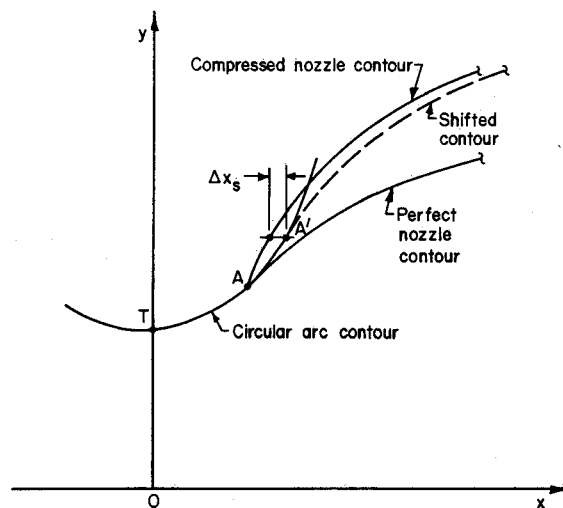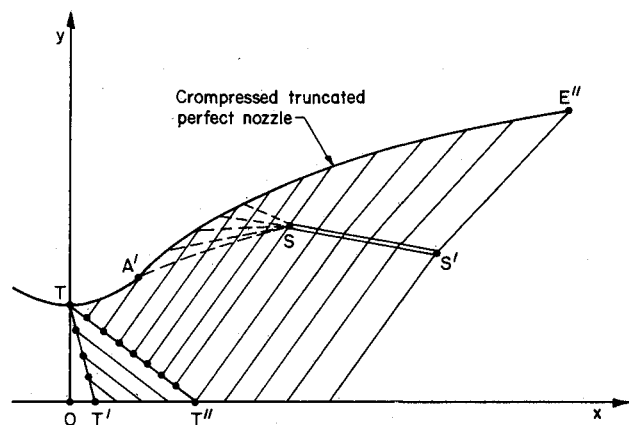
envelopes of the three Rao nozzles was also calculated and compared to the performance of the Rao nozzles. The gas thermodynamic properties, nozzle operating conditions, and nozzle throat contours were the same for all of the parametric studies. Table 1 presents a summary of those parameters.

Rao Nozzle Designs

The contour of Rao Nozzle 1 was furnished by Brown.[8] The area ratio of this nozzle was exactly 400. Rao Nozzles 2 and 3 were designed by an in-house program. That program selects points from the Mach line network emanating from the nozzle throat downstream circular arc contour as initial points, and solves the Rao[1] nozzle design equations to determine the exit left-running Mach line for the corresponding Rao nozzle. Consequently, the exit lip point cannot be specified a priori. If a specific length or area ratio is required, the program must be run in an iterative manner. For the parametric study, an exact area ratio was not required. Hence, Rao nozzles having area ratios close to the desired nominal area ratios of 200 and 100 were selected for use in the parametric study. Those area ratios were 190.43 and 97.32, respectively.

The specific impulses of the three Rao nozzles are presented in Table 2, along with the nozzle envelopes (i.e., lengths and area ratios). Those values are the reference values used in the parametric study.

Perfect Nozzle Designs

A set of 24 perfect nozzles, having area ratios from 97.32 to 800, was designed in the present study. These perfect nozzle designs formed the data base for the compressed truncated

perfect nozzle parametric study. The perfect nozzle contours were stored on disk and used as needed. The geometric properties and performances of these nozzles are summarized in Table 3.

Rao Nozzle 1 Studies

Rao Nozzle 1 had a length of 60.189 in., an area ratio of 400, and a specific impulse of 348.60 (lbf-s)/lbm. This nozzle was the reference nozzle for the studies presented in this section. From Table 3, the specific impulse of the perfect nozzle having an area ratio of 400 is 350.33 (lbf-s)/lbm.

A compressed truncated perfect nozzle was designed to fit the envelope of Rao Nozzle 1 by first truncating the perfect nozzle at an area ratio of 400 and then compressing the truncated perfect nozzle to a length of 60.189 in. The compressed truncated perfect nozzle was then analyzed to determine whether or not an oblique shock wave forms in the nozzle. If not, the performance was determined immediately. If enough right-running Mach lines coalesced to form an oblique shock wave, the origin of the shock wave was determined and the analysis was repeated accounting for the presence of the shock wave.

Only perfect nozzles having an area ratio equal to, or larger than, the area ratio of the reference Rao nozzle can be truncated to the area ratio of the reference Rao nozzle. Consequently, in the present study where the reference area ratio was 400, only the perfect nozzles presented in Table 3 having area ratios from 410 to 800 were considered.

Table 4 presents the performance of compressed truncated perfect nozzles designed to fit in the envelope of Rao Nozzle 1. The area ratio of the perfect nozzle is presented as the control parameter. The specific impulse I_{sp} of the compressed truncated perfect nozzles are presented. Shock waves occurred only in the two compressed nozzles corresponding to perfect nozzles having area ratios of 410 and 450. This trend was found throughout the entire parametric study. Sufficient compression to generate a shock wave only occurs for highly compressed nozzles.

The results presented in Table 4 are illustrated graphically in Fig. 5. Also presented in Fig. 5 for comparison are the performance of the perfect nozzle designed for an area ratio of 400 [350.33 (lbf-s)/lbm], Rao Nozzle 1 [348.60 (lbf-s)/lbm], the conical nozzle that fits in the envelope of Rao Nozzle 1 [342.79 (lbf-s)/lbm], and the 15 deg conical nozzle having the

same length as the Rao nozzle [342.43 (lbf-s)/lbm]. The optimum compressed truncated perfect nozzle corresponds to the perfect nozzle with an area ratio of approximately 650. It has a specific impulse of 348.02 (lbf-s)/lbm, which is 0.17% less than the specific impulse of the reference Rao nozzle [i.e., 348.60 (lbf-s)/lbm]. All of the compressed nozzles have a specific impulse less than the specific impulse of the reference Rao nozzle. Consequently, for this design envelope, the Rao nozzle is the best nozzle design.
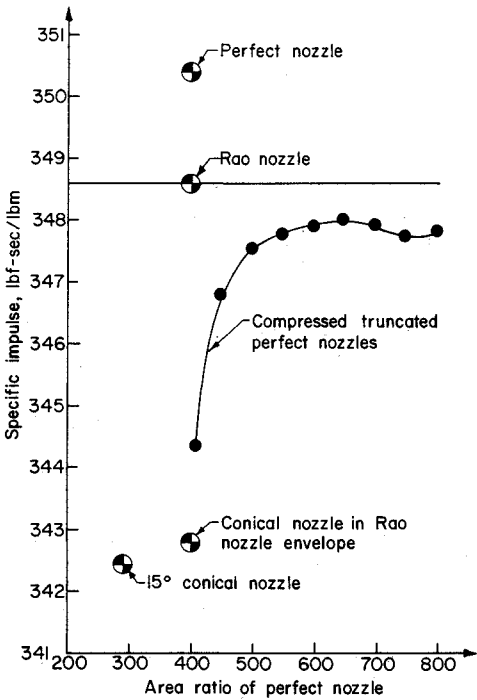

Fig. 5 Specific impulse of compressed nozzles designed to envelope of Rao Nozzle 1.

Table 4 Performance of compressed nozzles[a] designed to fit envelope of Rao Nozzle 1

$\epsilon_{perfect}$	I_{sp} lbf-s/lbm	Shock wave
410	344.35	yes
450	346.79	yes
500	347.53	no
550	347.77	no
600	347.89	no
650	348.02	no
700	347.92	no
750	347.75	no
800	347.82	no

[a]All of these nozzles have the same length and area ratio as Rao Nozzle 1, namely, $L = 60.189$ in. and $\epsilon = 400$.

Table 5 Performance of truncated perfect nozzles[a] designed to length of Rao Nozzle 1.

$\epsilon_{perfect}$	$\epsilon_{truncated}$	I_{sp} lbf-s/lbm
300	232.67	345.64
350	254.31	346.14
400	274.03	346.67
500	307.97	347.04
600	336.37	347.54
700	360.01	347.56
800	381.68	347.47

[a]All of these nozzles have the same length as Rao Nozzle 1, namely, $L = 60.189$ in., but a different area ratio.
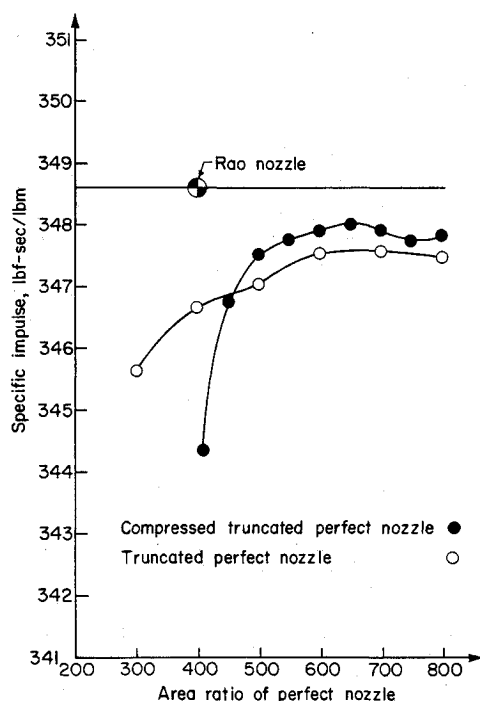
Table 3 Perfect nozzle geometric properties and performance

ϵ	θ_a, deg	L, in.	y_e, in.	I_{sp} lbf-s/lbm
97.32	27.237	61.986	9.823	337.56
100	27.3229	63.025	9.9573	337.85
112.5	27.6879	67.724	10.5615	339.09
125	28.0050	72.217	11.1330	340.17
150	28.5549	80.731	12.1958	341.97
175	28.9934	88.663	13.1734	343.43
190.43	29.2470	93.382	13.742	344.20
195	29.3147	94.742	13.906	344.42
200	29.3864	96.214	14.083	344.64
210	29.5227	99.114	14.431	345.08
225	29.7122	103.359	14.938	345.68
250	29.9948	110.183	15.746	346.58
300	30.4999	123.157	17.249	348.09
350	30.8984	135.232	18.632	349.31
400	31.2548	146.717	19.919	350.33
410	31.3184	148.937	20.166	350.51
450	31.5535	157.601	21.127	351.20
500	31.8120	167.996	22.270	351.96
550	32.0507	178.033	23.358	352.63
600	32.2678	187.725	24.397	353.23
650	32.4601	197.075	25.393	353.76
700	32.6339	201.131	26.352	354.25
750	32.7926	24.926	27.277	354.70
800	32.9385	223.486	28.172	355.11

Fig. 6 Comparison of compressed and truncated perfect nozzles for the envelope of Rao Nozzle 1.

Fig. 7 Specific impulse of $\epsilon = 600$ perfect nozzle truncated and compressed to length of Rao Nozzle 1.

An alternate design procedure simply truncates a series of perfect nozzle designs at a specified length and finds the best nozzle performance in this series of truncated perfect nozzles. The results of such a truncated perfect nozzle design study are presented in Table 5 and illustrated in Fig. 6. The specific impulse of the compressed truncated perfect nozzles are presented for comparison. Each truncated perfect nozzle has the same length as the reference Rao nozzle but a smaller area ratio. Consequently, each truncated perfect nozzle represents a different envelope. The optimum truncated perfect nozzle corresponds to the perfect nozzle with an area ratio of approximately 700. It has a specific impulse of 347.56 (lbf-s)/lbm, which is 0.30% less than the specific impulse of the reference Rao nozzle [348.60 (lbf-s)/lbm].

The performance curves of the compressed truncated perfect nozzles and the truncated perfect nozzles cross for the perfect nozzle having an area ratio of 450. For smaller perfect nozzles, the performance of the truncated perfect nozzles is considerably greater than the performance of the corresponding compressed truncated perfect nozzles. The shorter compressed nozzles are subject to the occurrence of oblique shock waves. This result suggests that the presence of the shock wave is not beneficial to nozzle performance, which is contrary to the principle behind the compressed truncated perfect nozzle concept proposed by Gogish.[3]

The final study concerned with Rao Nozzle 1 was a study in which the single perfect nozzle having a design area ratio of 600 was truncated at various area ratios and then compressed to the length of Rao Nozzle 1. The results of that study are presented in Table 6 and illustrated in Fig. 7. From these results, it is apparent that the reference Rao nozzle has a higher performance than all of the compressed nozzles. Interestingly, the best nozzle of this design series is the one truncated at the area ratio of the reference Rao nozzle and compressed to the length of the reference Rao nozzle. In other words, that nozzle fits exactly into the envelope of the reference Rao nozzle.

The parametric study using Rao Nozzle 1 as the reference nozzle clearly demonstrates that the Rao nozzle has higher performance than all of the compressed truncated perfect nozzles and all of the truncated perfect nozzles. The Rao noz-
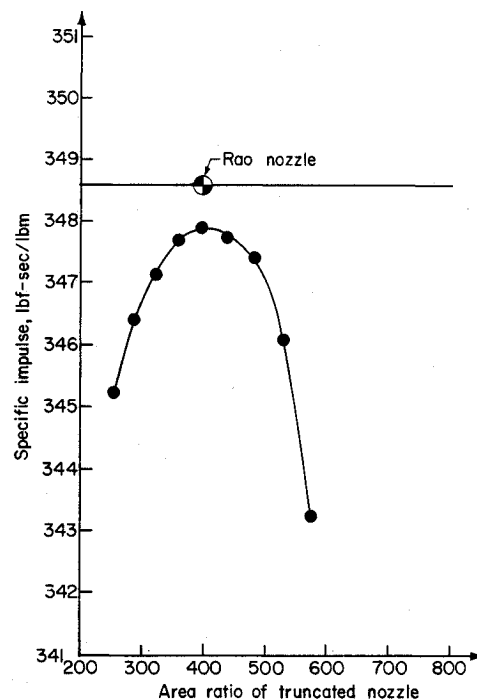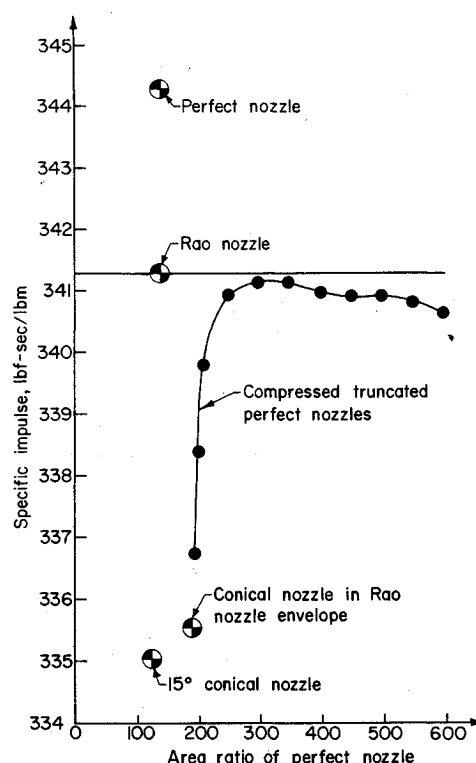

Fig. 8 Specific impulse of compressed nozzles designed to envelope of Rao Nozzle 2.

zle performance was only slightly better (0.17%) than the optimum compressed truncated perfect nozzle.

Rao Nozzle 2 Studies

Rao Nozzle 2 had a length of 38.255 in., an area ratio of 190.43, and a specific impulse of 341.29 (lbf-s)/lbm. This nozzle was the reference nozzle for the studies presented in this section. From Table 3, the specific impulse of a perfect nozzle having an area ratio of 190.43 is 344.20 (lbf-s)/lbm.

The same parametric study discussed above for Rao Nozzle 1 was conducted for Rao Nozzle 2. The results are presented in Figs. 8–10. The results obtained from this study are similar to the results obtained in the study of Rao Nozzle 1. The parametric study using Rao Nozzle 2 as the reference nozzle clearly demonstrates that the Rao nozzle has greater performance than all of the compressed truncated perfect nozzles and all of the truncated perfect nozzles. The Rao nozzle performance was only slightly better (0.04%) than the optimum compressed truncated perfect nozzle.

Rao Nozzle 3 Studies

Rao Nozzle 3 had a length of 24.567 in., an area ratio of 97.32, and a specific impulse of 333.45 (lbf-s)/lbm. This nozzle was the reference nozzle for the studies presented in this section. From Table 3, the specific impulse of a perfect nozzle having an area ratio of 97.32 is 337.56 (lbf-s)/lbm.

The same parametric study conducted for Rao Nozzles 1 and 2 was conducted for Rao Nozzle 3. The results are

Table 6 Performance of truncated $\epsilon = 600$ perfect nozzles[a] corresponding to Rao Nozzle 1 length

$\epsilon_{truncated}$	I_{sp} lbf-s/lbm	Shock wave
256	345.23	no
289	346.40	no
324	347.15	no
361	347.69	no
400[b]	347.89	no
441	347.76	no
484	347.42	yes
529	346.09	yes
576	343.23	yes
600	337.67	yes

[a] All of these nozzles have the same length as Rao Nozzle 1, namely, $L = 60.189$ in. [b] This truncated nozzle fits exactly into the envelope of Rao Nozzle 1.
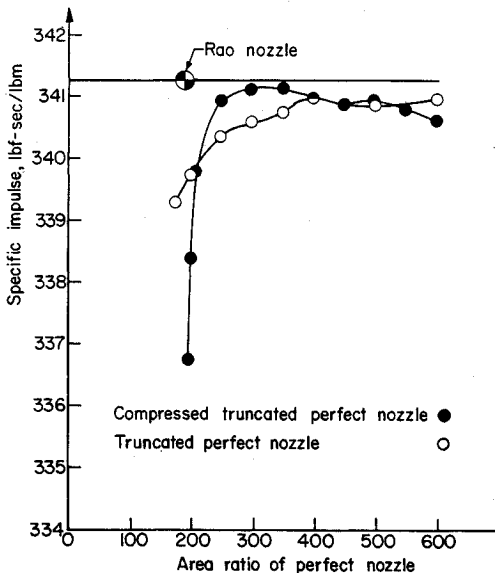

Fig. 9 Comparison of compressed and truncated perfect nozzles for the envelope of Rao Nozzle 2.
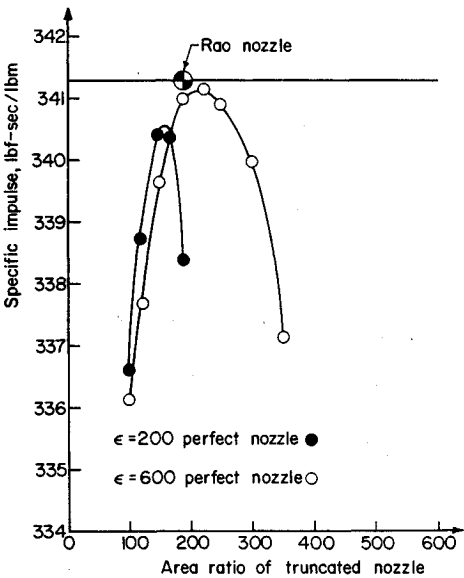

Fig. 11 Specific impulse of compressed nozzles designed to envelope of Rao Nozzle 3.

Fig. 10 Specific impulse of $\epsilon = 200$ and $\epsilon = 400$ perfect nozzle truncated and compressed to length of Rao Nozzle 2.
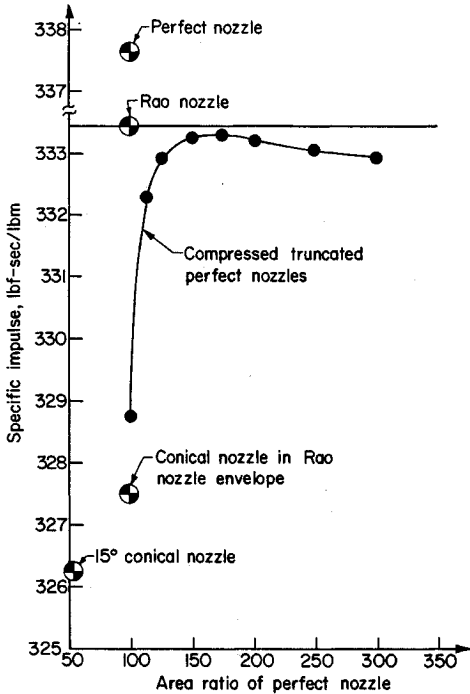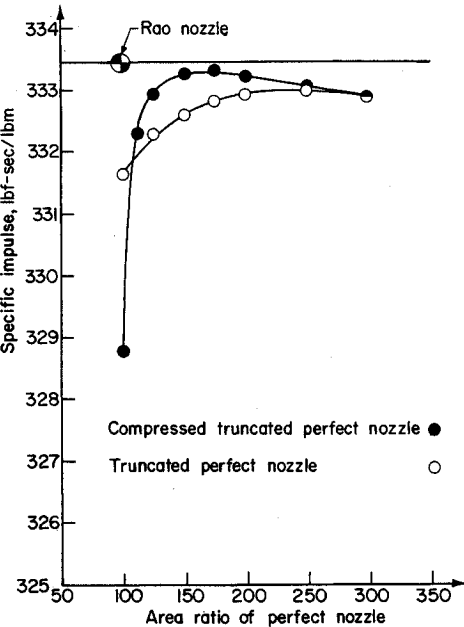

Fig. 12 Comparison of compressed and truncated perfect nozzles for the envelope of Rao Nozzle 3.
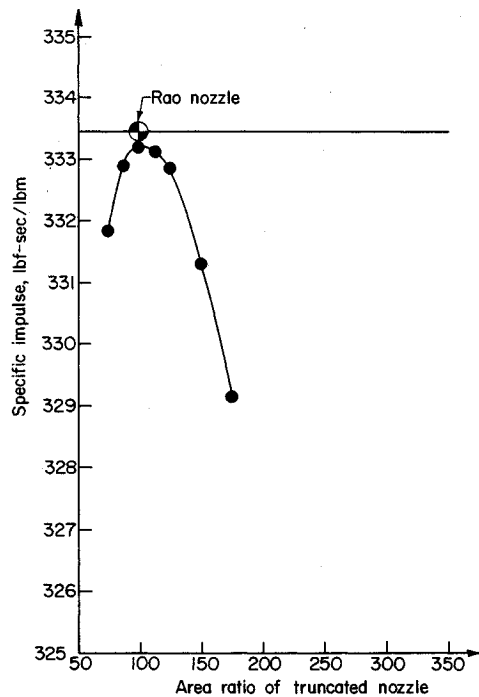
Fig. 13   Specific impulse of $\epsilon = 200$ perfect nozzle truncated and compressed to length of Rao Nozzle 3.

presented in Figs. 11-13. The results obtained from this study are similar to the results obtained in the study of Rao Nozzles 1 and 2. The parametric study using Rao Nozzle 3 as the reference nozzle clearly demonstrates that the Rao nozzle has greater performance than all of the compressed truncated perfect nozzles and all of the truncated perfect nozzles. The Rao nozzle performance was only slightly better (0.34%) than the optimum compressed truncated perfect nozzle.

Conclusions

An analysis is presented for designing and predicting the performance of compressed truncated perfect nozzles. A parametric study was conducted to determine the potential of compressed truncated perfect nozzles for use as propulsive nozzles. The results of that study show that in all cases the Rao nozzle has higher performance than compressed truncated perfect nozzles. Although the parametric study was of limited scope, it considered a wide range of area ratios, thus suggesting that the Rao nozzle design concept will always yield higher performing nozzles than the compressed nozzle design concept. For some designs, however, the difference in performance is quite small (0.04%), indicating that an optimum compressed truncated perfect nozzle is certainly a good propulsive nozzle. For envelopes (i.e., lengths and area ratios) for which the Rao nozzle procedure does not yield a design, the optimum compressed truncated perfect nozzle design procedure may yield highly efficient propulsive nozzle designs.

Acknowledgments

References

[1]Rao, G.V.R., "Exhaust Nozzle Contour for Maximum Thrust," *Jet Propulsion*, Vol. 28, June 1958, pp. 377-382.

[2]Ahlberg, J.H., Hamilton, S., Migdal, D., and Nilson, E.N., "Truncated Perfect Nozzles in Optimum Nozzle Design," *ARS Journal*, May 1961, pp. 614-620.

[3]Gogish, L.V., "Investigation of Short Supersonic Nozzles," *AN SSSR, Izvestiya, Mechanika Zhidkosti i Gaza*, 1966, No. 2, pp. 175-180.

[4]Zucrow, M.J. and Hoffman, J.D., *Gas Dynamics*, Vol. 2, John Wiley and Sons, New York, 1977, pp. 160-164.

[5]Kliegel, J.R. and Levine, J.N., "Transonic Flow in Small Throat Radius of Curvature Nozzles," *AIAA Journal*, Vol. 7, July 1969, pp. 1375-1378.

[6]Cline, M.C., "VNAP2: A Computer Program for Computation of Two-Dimensional, Time-Dependent, Compressible, Turbulent Flow," Rept. LA-8872, Los Alamos National Laboratory, Los Alamos, NM, Aug. 1981.

[7]Zucrow, M.J. and Hoffman, J.D., *Gas Dynamics*, Vols. I and II, John Wiley, New York, NY, 1977.

[8]Brown, S., Private communication, Air Force Rocket Propulsion Laboratory, Edwards Air Force Base, CA, Sept. 1983.